Investigations of magnetoelectric behavior in $BiFe_{0.95}Co_{0.05}O_3$ nanoparticles

V. G. Shrimali, Keval Gadani, K. N. Rathod, Hetal Boricha, Pooja Prajapati, M. J. Keshvani, B. R. Kataria, A. D. Joshi, D. D. Pandya, N. A. Shah, and P. S. Solanki

Citation: AIP Conference Proceedings **1837**, 040052 (2017); doi: 10.1063/1.4982136
View online: http://dx.doi.org/10.1063/1.4982136
View Table of Contents: http://aip.scitation.org/toc/apc/1837/1
Published by the American Institute of Physics

Investigations of Magnetoelectric Behavior in $BiFe_{0.95}Co_{0.05}O_3$ Nanoparticles

V.G. Shrimali[1,2], Keval Gadani[1], K.N. Rathod[1], Hetal Boricha[1], Pooja Prajapati[1], M.J. Keshvani[1], B.R. Kataria[3], A.D. Joshi[3], D.D. Pandya[4], N.A. Shah[1], P.S. Solanki[1,a)]

[1]*Department of Physics, Saurashtra University, Rajkot – 360 005, India*
[2]*Government Polytechnic, Rajkot – 360 003, India*
[3]*Department of Nanoscience and Advanced Materials, Saurashtra University, Rajkot – 360 005, India*
[4]*Human Resource Development Centre, Saurashtra University, Rajkot – 360 005, India*

[a)]Corresponding author: piyush.physics@gmail.com

Abstract. Nanophasic $BiFe_{0.95}Co_{0.05}O_3$ (BFCO) particles were synthesized using low cost, easy, simple, environment friendly and low temperature acetate precursor based modified sol–gel method. Influence of particle size and magnetic field on the structural, dielectric, impedance and a.c. conductivity of BFCO is investigated. X-ray diffraction (XRD) measurement has been performed to understand the structural modifications in the samples upon increasing the sintering temperature. Crystallite size (CS) increases from 33.62nm to 39.56nm due to agglomeration effect between the smaller crystallites. Effect of sintering temperature on the dielectric, impedance and conductivity has been studied and understood in the context of the creation of crystallite (particle) size and oxygen vacancies created due to high temperature sintering process. Magnetic field induced modifications in all these electrical properties [magnetoelectric (ME) effects] for the presently studied BFCO samples have been discussed on the basis of magnetostriction effect and charge mobility across the Fe–O lattice in the samples.

INTRODUCTION

Multiferroic materials show ferroelectric, anti/ferromagnetic and ferroelastic orderings within a single phase compound. Since multiferroics have interesting basic physics and potential applications, they have attracted a keen attention of researchers, scientists and engineers. [1–4]. Among all the multiferroic materials, $BiFeO_3$ (BFO) is the most promising due to its high Curie temperature (T_C) ~ 1103K and magnetic transition temperature (T_N) ~ 643K [5, 6]. Separate microscopic mechanisms are responsible for ferroelectricity and magnetism in BFO. Lone pairs of Bi^{+3} is responsible for the origin of the ferroelectricity while the magnetism arises due to the presence of localized electrons in partially filled d shell of transition metal [7]. However, there are some inherent drawbacks with BFO such as high leakage current and antiferromagnetic spiral spin structure with a periodicity ~ 62nm [8, 9]. This type of spin structure does not provide a net magnetization in bulk BFO. Thus, it is necessary to improve its properties for its practical application purpose. Some studies reveal that the reduction in particle size below 62nm gives rise to the suppression of spiral spin structure which improves the magnetic properties [10]. Besides the size effect at nanoscale, doping of transition metal ion at Fe site can also improve magnetic properties due to non exact compensation of magnetic moment and enhance dielectric properties due to reduction in valence fluctuations in Fe^{+3} [11].

Magnetoelectric (ME) effect is an significant feature of multiferroics that reveals the fact that charges can be controlled by the application of magnetic field and spins by applied voltage. It has been reported that the ME coupling appears directly between electric and magnetic order parameters or indirectly due to lattice strain [2]. The ME coupling is very small for most of the multiferroics at room temperature. Several strategies have been initiated

Functional Oxides and Nanomaterials
AIP Conf. Proc. 1837, 040052-1–040052-4; doi: 10.1063/1.4982136
Published by AIP Publishing. 978-0-7354-1507-2/$30.00

to enhance ME coupling at room temperature. Those strategies are (a) rare earth doping at A site or transition metal ion doping at B site in BFO and (b) synthesizing nanoparticles with crystallite size less than 62nm period of the spiral modulated spin structure [12–15]. Few reports are available on the observation of magnetodielectric (MD) response of transition metal ion doped $BiFeO_3$ system. 0.3% enhancement of MD constant was reported for Mn doped BFO by Yang et al [14]. Yadav et al [15] have reported ~ 6% MD response at room temperature in Ni doped BFO.

It has been observed that Co^{+3} doping at Fe^{+3} site in BFO can improve dielectric and magnetic properties but still MD effect has not been extensively studied in this compound [11]. On the basis of the above results, in this study, we discuss the effect of particle size on the structural, dielectric and MD properties of sol–gel grown Co doped BFO nanoparticles.

EXPERIMENTAL PROCEDURE

BFCO nanoparticles were prepared using low cost sol-gel method. All reagents were of analytical grade and were used without purification. Ferric nitrate Fe $(NO_3)_3 \times 9H_2O$, bismuth nitrate Bi $(NO_3)_3 \times 5H_2O$ and cobalt nitrate Co $(NO_3)_3 \times 6H_2O$ were taken in stoichiometric ratio. The precursor solution was prepared by dissolving constituents in double-distilled water and acetic acid which were taken in 1:1 molar ratio. After continuous stirring for few hours at 70ºC, the clear and transparent sol was completely turned in to brownish gel. Then, the gel was dried at 120ºC and grinded into powder. The powder was calcined at 350ºC for 6h. This as-prepared powder is pressed into pellet of 10mm in diameter. Finally, these pellets were sintered at 500 and 600ºC for 3h. The crystalline phases of the samples were determined by performing XRD measurement at room temperature using PANalytical PW3040/60 X'pert PRO diffractometer having Cu Kα radiation (λ = 1.54Å). Dielectric measurements were performed at room temperature under different magnetic fields using Agilent E4980A high-precision LCR meter in the frequency range of 20Hz–1MHz.

RESULTS AND DISCUSSION

Figure1 (a) XRD patterns of BFCO samples sintered at 500 and 600ºC revealing rhombohedral phase with space group R3c (no. 161) (JCPDS No. 71-2494). Besides the characteristic peaks of BFO, some other low intensity peaks of $Bi_{25}FeO_{39}$ phase are also observed, as indicated by asterisks in Fig.1 (a). Average CS of nanoparticles, obtained from the Scherer's formula [$CS = 0.9\lambda / \beta \cos\theta$, where β is full width at half maximum (FWHM) of the most intense peak, λ is the wavelength of X–rays used and θ is the Bragg angle]. FWHM decreases with increase in sintering temperature, suggesting the significant increase in crystallite size (CS). The value of CS increases with sintering temperature from 33.62nm (500ºC) to 39.56nm (600ºC). This can be due to crystal agglomeration effect where two or more crystallites combine and form larger one [16]. Any structural phase transition has not been observed with increase in sintering temperature. An enlarged view of most intense peak is shown in Fig.1(b) indicates better crystallinity at higher sintering temperature. The most intense peak shifts towards lower 2θ angle with increase in sintering temperature which is a indication of an enhancement in lattice parameters and hence in unit cell volume [17].

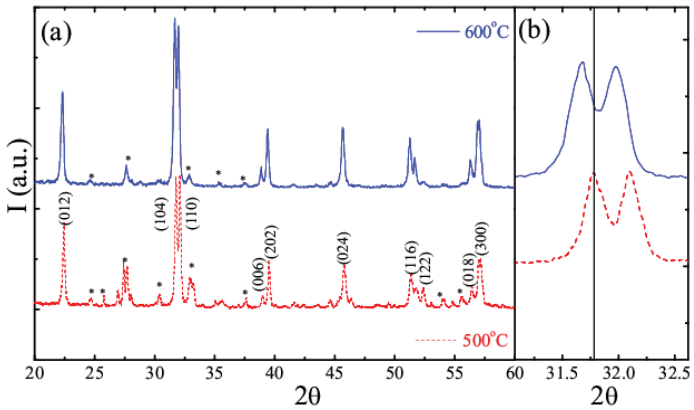

FIGURE 1. (a) XRD patterns of $BiFe_{0.95}Co_{0.05}O_3$ nanoparticles sintered at 500 and 600ºC and (b) enlarged view of most intense XRD peaks of BFCO nanoparticles.

Figure 2(left) shows frequency dependant behavior of dielectric constant (ε′) at room temperature under applied magnetic fields for BFCO samples sintered at 500 and 600°C. It can be seen that with increase in frequency, ε′ gets suppressed mainly due to relaxation of dipoles in high frequency region and their weak response towards applied electric filed. Also, at low frequencies, space charges are able to follow the frequency whereas at higher frequencies they do not follow the alteration of electric field [18]. It is found that the dielectric constant increases with increase in sintering temperature. This can be attributed to crystal agglomeration effect. As the sintering temperature increases crystal grows larger and porosity decreases. This type of dense and compact microstructure leads to improve dielectric constant [19]. Upon application of magnetic field of ~ 1.2T, dielectric constant increases for both the samples understudy. This suggests that BFCO nanoparticles exhibit positive MD effect [MD = $\{(\varepsilon_H - \varepsilon_0) / \varepsilon_0\} \times 100$]. Fig.2(right) shows calculated MD vs H plots (@ 1MHz) for presently studied BFCO nanoparticles. With increase in magnetic field, MD increases for both the samples. In addition, MD is almost six times larger in 500°C sintered sample as compared to 600°C sintered sample. This can be understood as: while applying magnetic field, it creates magnetostriction effect, thereby, produces the strain in the BFCO system which enhances the polarization of the dipoles.

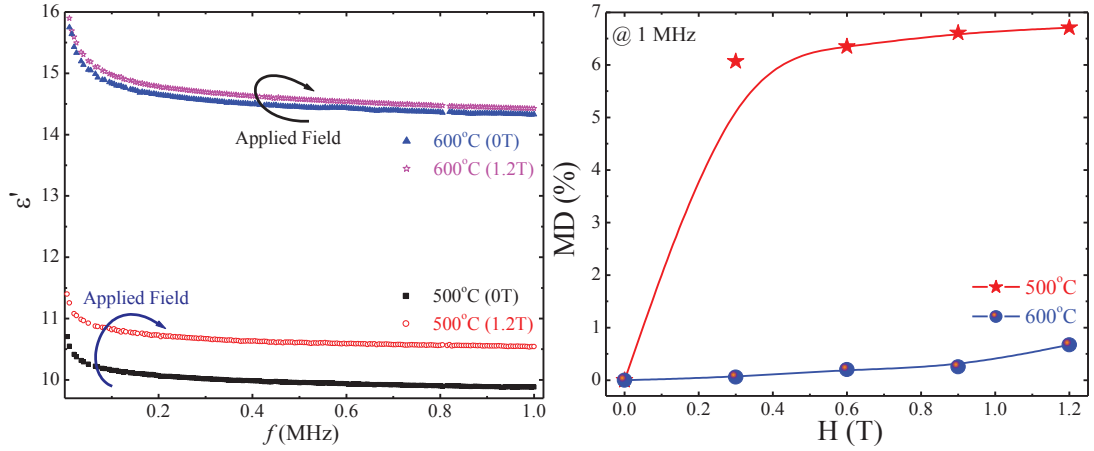

FIGURE 2. (left) Frequency dependant dielectric constant under zero and 1.2T applied magnetic fields and (right) magnetic field dependant magnetodielectric (MD) for $BiFe_{0.95}Co_{0.05}O_3$ nanoparticles sintered at 500 and 600°C.

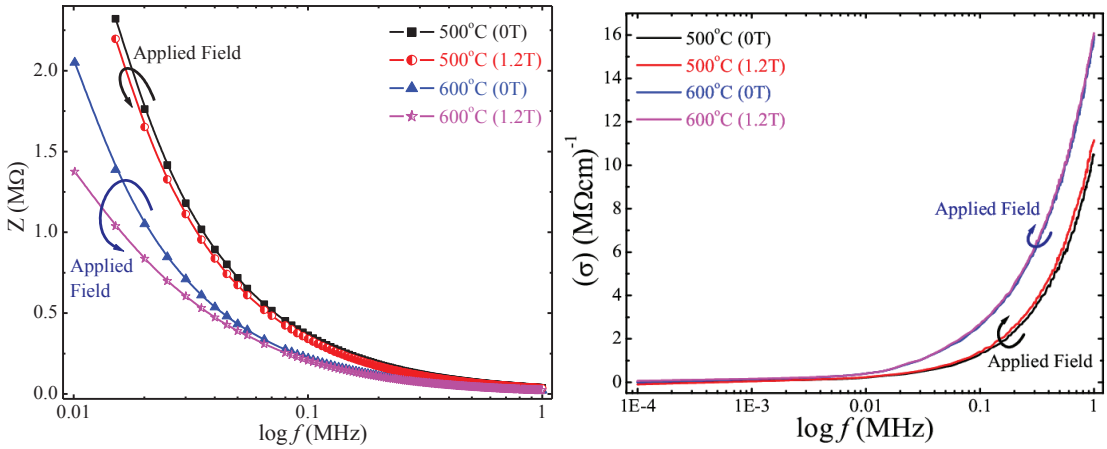

FIGURE 3. (left) Frequency dependant impedance under zero and 1.2T applied magnetic fields and (right) Frequency dependant a.c. conductivity under zero and 1.2T applied magnetic fields for $BiFe_{0.95}Co_{0.05}O_3$ nanoparticles sintered at 500 and 600°C.

Figure 3(left) shows the variation in impedance with frequency for both the BFCO samples under zero and 1.2T applied magnetic fields revealing a typical reduction in impedance with frequency. With increase in sintering temperature, impedance gets suppressed throughout the frequency range studied. This can be understood on the basis of oxygen vacancy created naturally in the samples upon sintering process [20]. It is reported that with increase in sintering temperature, oxygen vacancy is increased [20]. For the present case of BFCO nanoparticles, 600°C

sintered sample possesses large number of oxygen vacancy as compared to lower temperature sintered sample. Oxygen vacancies concentration creates variation in oxidation states of Fe ions (between Fe^{+2} and Fe^{+3}) in the samples. Co–existance of Fe^{+2} and Fe^{+3} in octahedral sites enhances the electron transfer between Fe^{+2} and Fe^{+3} via oxygen ions [21], thereby reducing the impedance upon enhancing the sintering temperature. Upon application of magnetic field of 1.2T, impedance is suppressed throughout the frequency range studied which can be due to the field induced improved spin structure of Fe ions and hence electronic transfer across the Fe–O lattice. Magnetoimpedance (MI) [$MI = \{(Z_H - Z_0) / Z_0\} \times 100$] is found to be negative, i.e. suppression in impedance upon the application of magnetic field, for both the samples understudy. Fig.3(right) shows the variation in a.c. conductivity with frequency under zero and 1.2T applied magnetic fields for both the BFCO samples sintered at different temperatures. Conductivity is found to increase exponentially with increase in frequency as well as with sintering temperature. This can also be understood in terms of oxygen vacancies created due to different sintering temperatures, as discussed above. Magnetoconductivity (MC) can be calculated using the formula: $MC = \{(\sigma_H - \sigma_0) / \sigma_0\} \times 100$. In contrast to the magnetoimpedance (MI) effect, MC is found to be positive in nature for both the BFCO samples.

CONCLUSIONS

In conclusion, the structural, electrical and magnetoelectric (ME) properties of BFCO nanoparticles have been investigated. Nanophasic BFCO samples were grown using cost effect acetate precursor based modified sol–gel method. Effect of sintering temperature on dielectric behavior has been understood in the context of crystallite size while modifications in the impedance and a.c. conductivity have been discussed in the light of oxygen vacancies created in the samples sintered at different temperatures. Magnetoelectric effect, i.e. magnetic field induced modifications in these electrical properties, has been understood by magnetostriction effect and controlled charge transfer across the Fe–O lattice in the samples understudy.

REFERENCES

1. M. Fiebig, *J. Phys. D: Appl. Phys.* **38**, R123–R152 (2005).
2. W. Eerenstein, N. D. Mathur and J. F. Scott, *Nature (London)* **442**, 759–765 (2006).
3. S. W. Cheong and M. Mostovoy, *Nature Mater.* **6**, 13–20 (2007).
4. R. Ramesh and N. A. Spaldin, *Nature Mater.* **6**, 21–29 (2007).
5. M. Mahesh Kumar, V. R. Palkar, K. Srinivas and S. V. Surynarayana, *Appl. Phys. Lett.* **76**, 2764–2766 (2000).
6. J. M. Moreau, C. Michel and W. J. James, *J. Phys. Chem. Solids* **32**, 1315–1320 (1971).
7. D. I. Khomskii, J. Mag. Mag. Mater. **306,** 1–8 (2006).
8. X. D. Qi, J. Dho, R. Tomov, M. G. Blamire and J. L. MacManus–Driscoll, *Appl. Phys. Lett.* **86**, 062903:1–3 (2005).
9. C. Ederer and N. A. Spaldin, *Phys. Rev. B* **71**, 060401:1–4 (2005).
10. F. Gao, Y. Yuan, K. F. Wang, X. Y. Chen, F. Chen, J. M. Liu and Z. F. Ren, *Appl. Phys. Lett.* **89**, 102506:1–3 (2006).
11. K. Chakrabarti, B. Sarkar, V. D. Ashok, S. S. Chaudhari and S. K. De, *J. Mag. Mag. Mater.* **381**, 271–277 (2015).
12. A. Mukherjee, S. Basu, P. K. Manna, S. M. Yusuf and M. Pal, *J. Mater. Chem. C.* **2**, 5885–5891 (2014).
13. H. M. Jang, J. H Park, S. Ryu and S. R. Shannigrahi, *Appl. Phys. Lett.* **93**, 252904:1–3 (2008).
14. C. H. Yang, T. Y. Koo and Y. H. Jeong, *Solid State Commun.* **134**, 299–301 (2005).
15. K. L.Yadav and Amit Kumar, *Phys. B* **405**, 4650–4654 (2010).
16. Megha Vagadia, Ashish Ravalia, Uma Khachar, P. S. Solanki, R. R. Doshi, S. Rayaprol and D. G. Kuberkar, *Mater. Res. Bull.* **46**, 1933–1937 (2011).
17. D. G. Kuberkar, R. R. Doshi, P. S. Solanki, Uma Khachar, Megha Vagadia, Ashish Ravalia and V. Ganesan, *Appl. Sur. Sci.* **258**, 9041–9046 (2012).
18. H. O. Rodrigues, G. F. M. Pires Jr., J. S. Almeida, E. O. Sancho, A. C. Fereira, M. A. S. Silva and A. S. B. Sombra, *J. Phys. Chem. Solids* **71**, 1329–1336 (2010).
19. X. Z. Chen, R. L. Yang, J. P. Zhou, X. M. Chen, Q. Jiang and P. Liu, *Solid State Sci.* **19**, 117–121 (2013).
20. N. A. Shah, *Appl. Nanosci.* **4**, 889–895 (2014).
21. S. Hunpratub, P. Thongbai, T. Yamwong, R. Yimnirun, S. Maensiri, *Appl. Phys. Lett.* **94**, 062904:1–3 (2009).